A CASE STUDY OF THE CLAYCOMO, MISSOURI MICROBURST ON JULY 30, 1989 *

Paul J. Biron, Mark A. Isaminger, Kevin J. Flemming
M.I.T. Lincoln Laboratory
Lexington, Massachusetts 02173

Alan A. Borho
University of North Dakota, Center for Aerospace Sciences
Grand Forks, North Dakota 58202

1. INTRODUCTION

The Terminal Doppler Weather Radar (TDWR) testbed collected thunderstorm measurements in the Kansas City area from March 27 through October 6, 1989. Of the 393 microbursts detected by the radar, 21 were classified as severe, with a differential velocity > 24 m/s. None of the severe events impacted terminal operations at Kansas City International Airport (KCI). Nevertheless, there were 42 microbursts within 3 nautical miles of the airport.

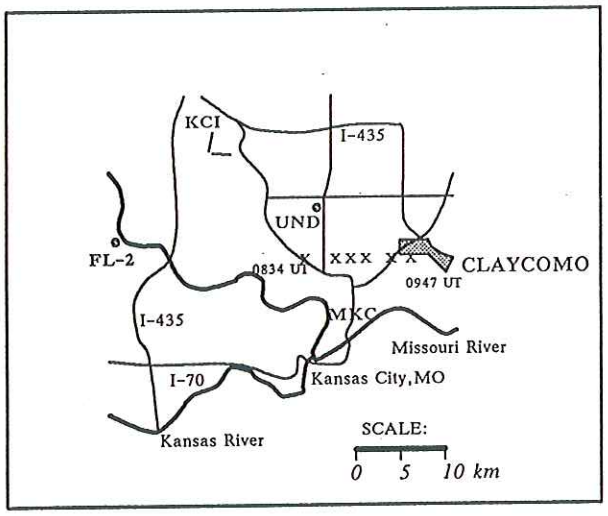

Figure 1. Map of the Kansas City area showing the track (x) of the Claycomo microburst producing cell in 15 minute intervals.

2. CASE STUDY

In this paper, a microburst that occurred on July 30, 1989 near Claycomo, Missouri (see Figure 1) will be examined. The outflow damaged trailers and uprooted trees in the area. Winds in excess of 55 mph, pea-sized hail, and 3 1/2 inches of rain accompanied the storm. This was the strongest microburst observed during the 1989 data collection season in Kansas City.

On July 30, microburst outflows were first detected northwest of the downtown airport (MKC) at 0709 UT and east of the University of North Dakota (UND) radar at 0806 UT. The echo which produced the Claycomo microburst developed at 0820 UT in the vicinity of the earlier outflows. It attained a maximum storm top height in excess of 15 km AGL.

2.1. Radar Data

Figure 2 is a radial velocity plot from FL-2 at the time of the maximum outflow. The wind shear is centered 29 km and 91° azimuth from the radar (A).

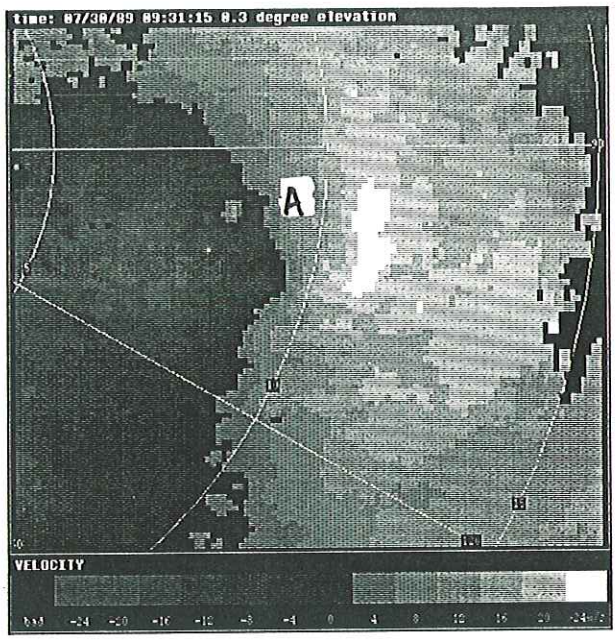

Figure 2. FL-2 radar velocity plot at 09:30:51 UT, the time of maximum outflow strength. Range rings are labelled in km.

Figure 3 is a synthesized vertical cross section plot (RHI) of the storm cell for velocity. This RHI was generated along the 91.5° azimuth and shows the maximum outflow (A in figure 3) and vertical structure of the storm. Convergence can be seen at approximately 2 km above the surface (B in figure 3). The RHI was created from available PPI data using scans ranging from 0.4° to 39.9° elevation. Gaps between consecutive tilts were then filled using a Cressman weighting interpolation technique.

*The work described here was sponsored by the Federal Aviation Administration. The United States Government assumes no liability for its content or use thereof.

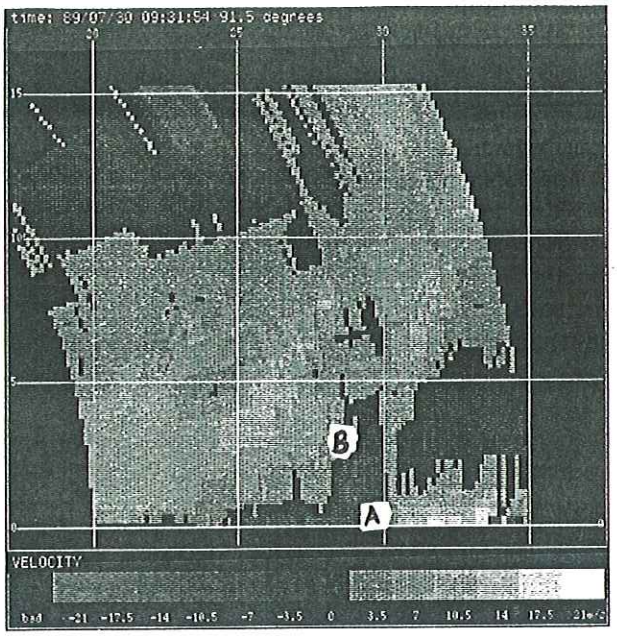

Figure 3. FL–2 radar velocity vertical cross section along 91.5 degrees at 09:31:57 showing the maximum outflow. Grid lines indicate height and range from FL–2 in km.

The microburst persisted for approximately 1 hour, with a peak differential velocity observed by FL–2 of 38 m/s over 4 km at 300 meters above ground level (AGL). A radial velocity plot from UND at 0931 UT (Figure 4) suggests that

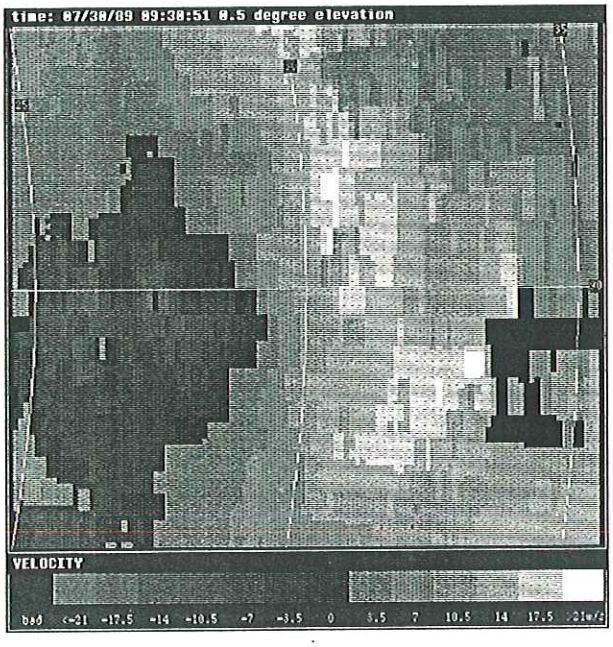

Figure 4. UND radar velocity plot showing the maximum outflow strength at 70 m AGL. Range rings are labelled in km.

the outflow was stronger at lower levels since UND recorded a peak differential velocity of 45 m/s over 3 km at a height of 70 meters AGL. The peak shear was observed on the first available surface scan from UND.

2.2. Microburst Features

Figures 5a and 5b present a summary of the velocity features aloft and reflectivity features observed by the FL–2 radar throughout the life cycle of the microburst. These features were manually extracted from the radar data to correspond with those expected as microburst precursors by the automated TDWR microburst detection algorithm (Campbell 1989). The initial time of the microburst outflow is represented by T = 0. The microburst reached its peak velocity differential of 38 m/s at T + 42 minutes (indicated by the heavy vertical line in each plot). Upper level divergence first occurred at T – 15 minutes and reached a peak intensity of 25 m/s at T + 37.5 minutes. Anticyclonic rota-

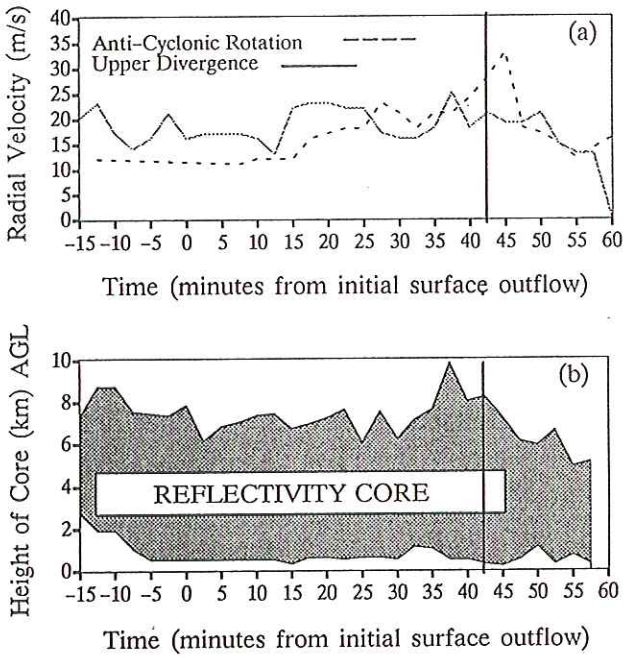

Figure 5. (a) Velocity features aloft observed throughout the life cycle of the Claycomo microburst. (b) Height of the reflectivity core throughout the life cycle of the Claycomo microburst.

tion is first observed at T – 13 minutes; however, this feature is not consistently observed until after the initial microburst outflow. It reaches a maximum intensity of 32 m/s over 1° azimuth. At a distance of 30 km, this represents a single–Doppler vorticity of 61 x 10^{-3} s^{-1}. The rotation produced in this downdraft is comparable to the vertical vorticity of a misocyclonic microburst observed in Colorado (Kessinger et al. 1984). The severity of this microburst could have been predicted by the increase in the depth of the reflectivity core

and the intensity and trend of mid- and upper-level features such as anticyclonic rotation and upper-level divergence.

2.3. Liquid Water Based Measures

The average vertically integrated liquid water (VIL) was estimated at a 45 dBZ contour using a prototype algorithm based on Greene and Clark (1972). The volume of integration was the three-dimensional structure based on the 45 dBZ storm boundary (Figure 6) which is recognized by the TDWR microburst detection algorithm as described in Merritt et al. (1989). The integration method uses a volume weighted average of estimated liquid water content in the two-dimensional (tilt) regions followed by midpoint integration in elevation. The average VIL (as shown in Figure 7b) is then calculated by dividing the mass by the cell's area.

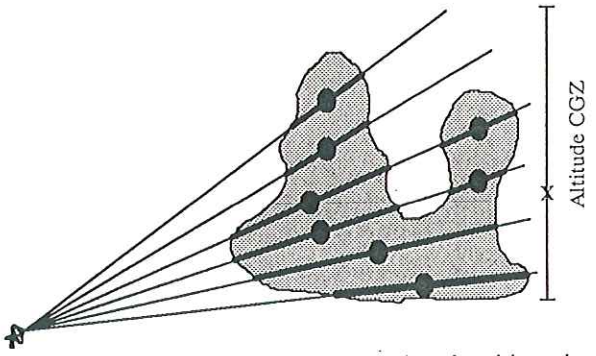

Figure 6. An example of a the reflectivity regions found in a cloud, their centroids, and the resulting CGZ.

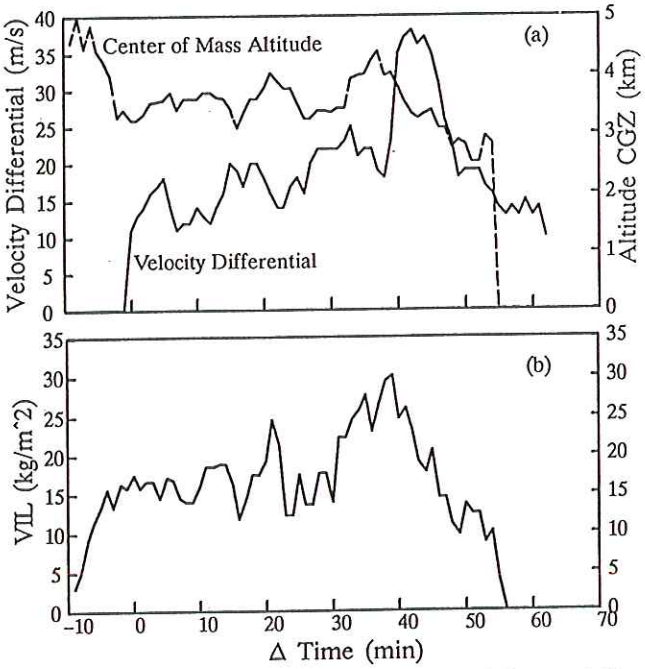

Figure 7. (a) Velocity Differential and Altitude of Center of Mass (CGZ) @ 45dBZ contour vs. ΔTime (b) VIL (@45 dBZ contour) vs ΔTime for Claycomo, Missouri microburst on July 30, 1989. T=0 is 084828 UT.

The altitude of the center of mass (CGZ) shown in Figure 7a was estimated at the 45 dBZ contour. As shown in Figure 6, 45 dBZ regions whch overlap are associated together by the TDWR microburst detection algorithm. The CGZ is calculated as follows:

$$CGZ = \frac{\sum M_i Z_i}{\sum M_i}$$

where M_i are the masses of the individual regions and Z_i are their altitudes, with i denoting the particular region. Because the regions actually represent a wedge shaped section of space, this does not give a true center of gravity (the estimate will always be low), but it is a good first-order estimate.

Figure 8 is a time series of contour plots of this storm's reflectivity. Figure 8a is 11° PPIs which were selected to reveal the storm structure at 5 km AGL. Figures 8b and 8c are time series of synthesized RHIs at two different azimuths in the storm which shift in order to track significant features at different times. Figure 8d is the FL-2 radial velocity differential through the surface outflow plotted to the same time scale.

By examining this figure we can see that this was a complex multicell storm. The pulses in surface velocity differential can be associated with distinct sub-events in the storm evolution. Cell growth appeared on the western flank while cells collapsed to the east. The center of divergence was closely correlated in both time and space to the collapsing cells.

The TDWR microburst detection algorithm associates all of these sub-events into one large event because of the high reflectivity of the cells and their close proximity. The CGZ product was not able to resolve all of these sub-events, but it does show a pulsing behavior before each major pulse in the surface outflow, with descents at times -6, 13, 21, and 37 minutes. These descents preceded the surface velocity differential with mean lead times of 2.5 minutes for pulse onset and 7.5 minutes for pulse peak. We believe the increases in CGZ prior to the descents were caused by 1) formation of new precipitation aloft and 2) a loss of precipitation loading from the bottom of the storm from a previous cell's collapse. The descents of CGZ were made apparent by their preceding increases; it is not clear whether CGZ would be effective in identifying these sub-events, and thus anticipating pulses in velocity, in other multicell storms.

The average VIL reached its peak 3 minutes before the peak outflow. It does not appear to be a good predictor for the timing of the pulses in this microburst. However, it was a good predictor of the strength of these pulses. The VIL values calculated at the beginning of each core descent (as sensed by CGZ descent) were 12, 19, 25, and 27 kg/m^2. The peaks of the subsequent divergence pulses were 18, 20,

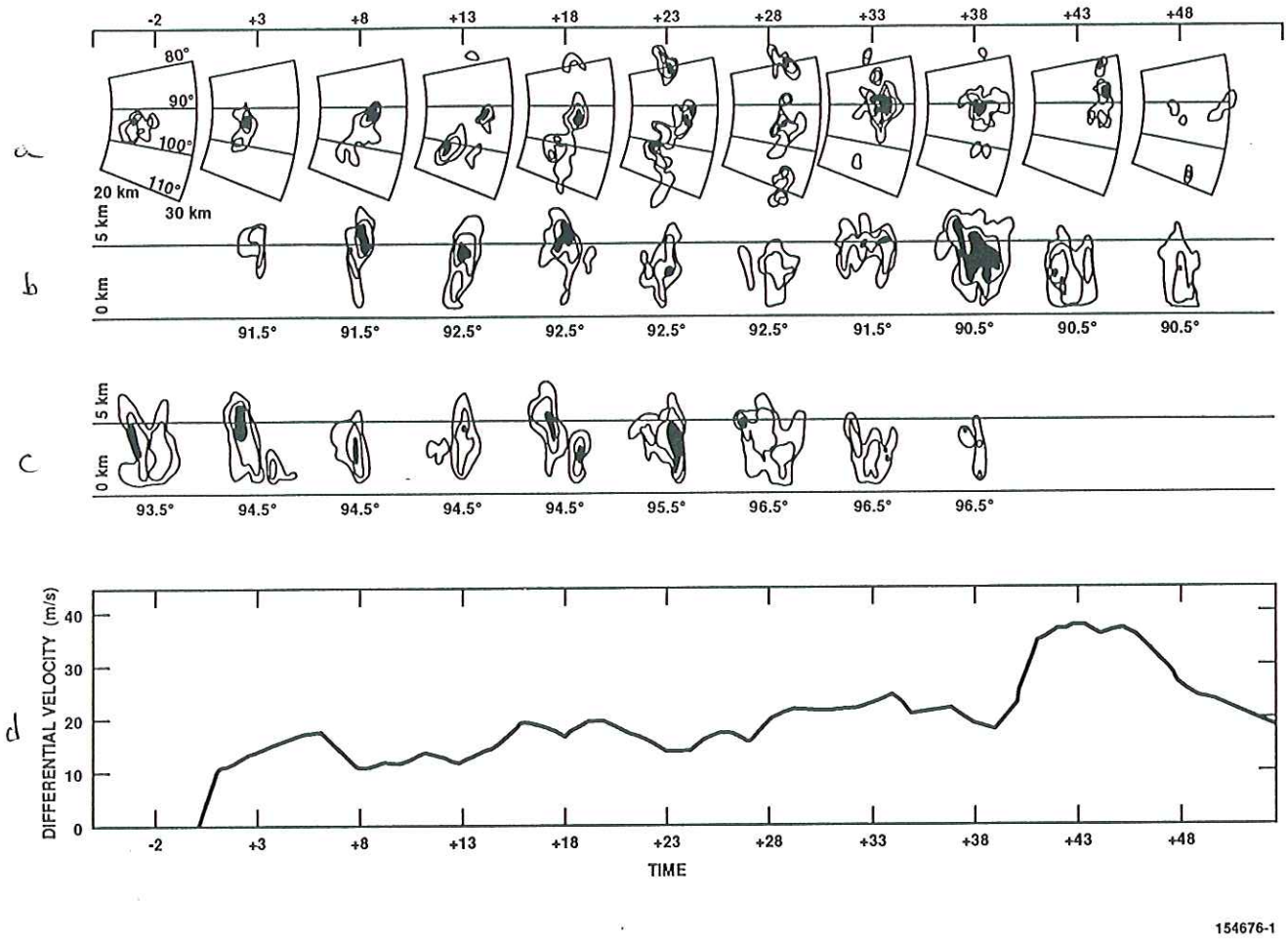

Figure 8. (a) Time series of 11° PPIs with contours at 45 and 50 dBZ. Solid areas are above 55 dBZ.
(b) and (c) synthetic RHIs at selected azimuths through the storm. The contours and time scale are the same as in the PPIs shown in (a).
(d) FL-2 surface velocity differential magnitude (m/s) plotted to the same time scale.

25 and 38 m/s. Thus, higher VIL values were associated with greater surface velocity differentials.

2.4. Aircraft Hazard Index

Figure 9 is a plot showing ΔV and ΔV/ΔR throughout the life cycle of the microburst. It can be seen from this plot that the maximum ΔV/ΔR was not coincident with the time of maximum ΔV. The event pulsed a number of times prior to dissipation. In fact, the ΔV of the outflow was greater with each subsequent pulse.

An assessment of how this microburst would have affected an aircraft's performance can be made by considering the F-factor, a derived quantity which characterizes the effect of a wind shear encounter on the flight performance of an aircraft as a function of ΔV/ΔR. Targ and Bowles (1988) define the F-factor as:

$$F = \frac{\frac{Dv_x}{Dt}}{g}\cos\gamma + \frac{\frac{Dv_z}{Dt}}{g}\sin\gamma - \frac{W}{TAS}$$

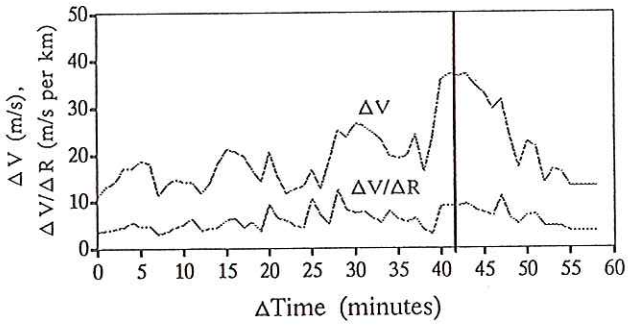

Figure 9. ΔV/ΔR (m/s per km) and ΔV (m/s) vs. ΔTime (min.) (FL-2) for the Claycomo, Missouri microburst on July 30, 1989. T=0 is 084828 UT. The heavy vertical line indicates the time of maximum surface outflow.

where γ is the flight path angle, TAS is the true air speed of the aircraft, g is the gravitational constant of acceleration, and W is the vertical wind velocity. The substantial derivative with respect to time is given by:

$$\frac{Dv_x}{Dt} = \frac{\delta v_x}{\delta t} + V_h \frac{\delta v_x}{\delta x} + V_v \frac{\delta v_x}{\delta z}$$

where V_h is the horizontal component of the aircraft velocity, V_v is the vertical component of the aircraft velocity, and $\delta v_x/dx$ and $\delta v_x/dz$ are the horizontal and vertical components of the wind, respectively, along the flight path of the aircraft. Assuming a "frozen" wind field in time, stable flight ($\gamma = 0$), and V_h = TAS, the F-factor is approximated by:

$$F = \frac{TAS \dfrac{\delta V_x}{\delta x}}{g} - \frac{W}{TAS}$$

In a paper by Elmore and Sand (1989), F-factor was plotted as a function of $\Delta V/\Delta R$ for 39 microbursts. In their analysis, a TAS of 75 m/s was used in the space-to-time conversion from $\Delta V/\Delta R$ to Dv_x/Dt. W is estimated from a sine wave model of divergent outflow. An F-factor of 0.13 is said to be the nominal value for aircraft performance to be marginal for level flight.

In the case of the Claycomo microburst, the maximum $\Delta V/\Delta R$ of 12.2 m/s per km would correspond to an F-factor of 0.186, significantly above the hazard threshold of 0.13 (indicated by the horizontal line in Figure 10). Figure 10 is a plot of F-factor throughout the life history of the microburst. It can be seen that the F-factor peaked above the hazard threshold five separate times and remained above this threshold for four minutes at the time of maximum ΔV. The maximum $\Delta V/\Delta R$ of 14.1 m/s per km as seen by the UND radar (not plotted) would correspond to an F-factor of 0.21(X in figure 10), a considerable hazard to an aircraft penetrating the outflow. This is comparable to the F-factor calculated for a hazardous microburst windshear on July 11, 1988 at Denver's Stapleton Airport (Schlickenmaier, 1989). Due to scanning strategy, UND data is only available from 093115 UT through 094307 UT (41 to 47 minutes).

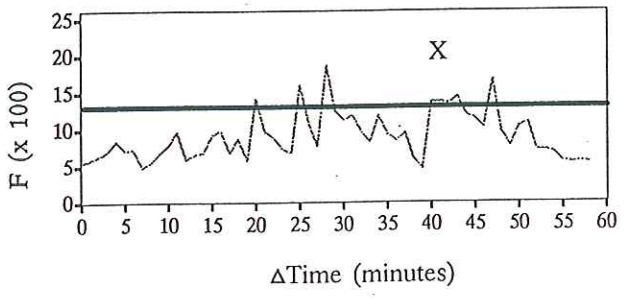

Figure 10. F-factor vs. ΔTime (Fl-2) for the Claycomo, Missouri microburst on July 30, 1989. T=0 is 084828 UT. X corresponds to the UND peak F-factor

3. CONCLUSION

On July 30, 1989, a strong multicell thunderstorm near Claycomo, Missouri produced a microburst with a maximum differential velocity of 45 m/s. This was the strongest microburst observed during the 1989 data collection season in Kansas City. The microburst was preceded by mid- and upper-level velocity features as well as a descending high reflectivity core. For this case, each surface velocity differential pulse was preceded by a descent in CGZ. The average VIL at the beginning of the CGZ descent was a good predictor of the ranking of the surface velocity differential pulse magnitudes. An analysis of the maximum $\Delta V/\Delta R$ and F-factor revealed that this microburst would have been a considerable hazard to an aircraft penetrating the outflow.

ACKNOWLEDGEMENTS

The authors would like to thank Dr. James Evans, Dr. Marilyn Wolfson, Cynthia Engholm, and Seth Troxel for their editorial comments and meteorological insight. We would also like to acknowledge Douglas Piercey of the FL-2 radar and the UND radar crew whose efforts in the early morning of July 30 helped make this work possible.

REFERENCES

Campbell, S., 1989: "Use of Features Aloft in the TDWR Microburst Recognition Algorithm," 24th Conference on Radar Meteorology, Tallahasee, FL.

Elmore, K. and W. Sand, 1989: "A Cursory Study of F-Factor Applied to Doppler Radar," 3rd International Conference on the Aviation Weather System, Anaheim, CA.

Greene, D. and R. Clark, 1972: "Vertically Integrated Liquid Water -- A New Analysis Tool," *Monthly Weather Review*, **100**, 548-552.

Kessinger, C.J., J.W. Wilson, M. Weisman and J. Klemp, 1984: "The Evolution of Misoscale Circulations in a Downburst Producing Storm and Comparison to Numerical Results," 22nd Conference on Radar Meteorology, Zurich, Switzerland.

Merritt, M., D. Klingle-Wilson, and S. Campbell, 1989: "Wind Shear Detection with Pencil-Beam Radars," *The Lincoln Laboratory Journal*, 2, 483-510.

Schlickenmaier, H.W., 1989: "Windshear Case Study: Denver, Colorado, July 11, 1988," FAA Technical Report DOT/FAA/DS-89/19.

Targ, R. and R Bowles, 1988: "Investigation of Airborne Lidar for Avoidance of Windshear Hazards," AIAA Conference on Sensor and Measurement Techniques for Aeronautical Applications, Atlanta GA.